Ocean Engineering 312 (2024) 119258

Contents lists available at ScienceDirect

Ocean Engineering

journal homepage: www.elsevier.com/locate/oceaneng

Research paper

Hull-propeller-rudder interactions: Time-accurate data of a scaled model ship in waves

Stephen Turnock [a], Saeed Hosseinzadeh [a], Yifu Zhang [a,b,*], James Bowker [a,c], Dickon Buckland [d], Magnus Gregory [d], Nicholas Townsend [a]

[a] Maritime Engineering, University of Southampton, Boldrewood Campus, Southampton, SO16 7QF, Hampshire, UK
[b] High Performance Computing (HPC) Team, University of Southampton, Highfield Campus, Southampton, SO17 1BJ, Hampshire, UK
[c] QinetiQ, Haslar Marine Technology Park, Gosport, PO12 2AG, Hampshire, UK
[d] Wolfson Unit for Marine Technology and Industrial Aerodynamics, University of Southampton, Boldrewood Campus, Southampton, SO16 7QF, Hampshire, UK

ARTICLE INFO

Keywords:
Free running model tests
Model testing
Testing facilities
Synchronised measurements
Hull-propeller-rudder interaction
Energy efficiency
Experimental uncertainty

ABSTRACT

Accurate prediction of ship powering performance is essential as it plays a pivotal role in achieving optimal ship design and maximising energy-saving potential. Typically, a combination of computational and experimental methods is employed. With great progress in the use of computational simulations, there is an equivalent need to acquire high-quality experimental measurements and insights gained from towing tank tests. This paper introduces a newly constructed, instrumented geosim of the benchmark KRISO Container Ship (KCS) hull form and details representative results from four distinct test campaigns that encompass both free-running and towed conditions. These tests were conducted in calm water, regular waves, and irregular waves, with evaluations at various drift angles to thoroughly assess the hull's performance under different maritime conditions. The synchronised measurements of wave environment, model motions, forces and moments of the hull and its appendages, facilitate a time-accurate understanding of performance, rather than merely capturing average behaviour. This provides a deeper insight into the complex interactions between the hull, propeller, and rudder, and how that affects the power demand in real voyages. The collected data from experiments helps validate CFD codes and also observe real physics, which is impossible from any virtual test run with numerical simulations.

1. Introduction

The ambition to decarbonise the shipping sector by 2050 significantly amplifies the urgent need for enhanced energy efficiency, as emphasised in MEPC72 (2018). This requires a more in-depth comprehension of the hydrodynamic behaviour and powering performance of ships when navigating through waves (Molland et al., 2017). Such insights are of high importance not only for boosting propulsive energy efficiency of vessels but also for minimising greenhouse gas emissions, all while ensuring the continued safety and reliability of maritime operations. Accurately predicting ship hydrodynamics in wave conditions is complex due to the overlapping interactions among ship resistance, propulsion, seakeeping, manoeuvrability, and ship hydroelasticity. These interactions are further complicated by varying wave conditions. More specifically, wave conditions introduce nonlinear effects such as changes in wave height and frequency, which can drastically alter the hydrodynamic forces experienced by the ship. Meanwhile, seakeeping introduces dynamic effects like slamming, where waves impact the ship's hull with significant force, and whipping, which involves rapid structural vibrations following a slamming event. Additionally, hydroelastic effects such as springing, where the ship's structure undergoes cyclic stresses due to wave-induced vibrations, further challenge the predictive modelling of ship behaviour in waves (Hirdaris and Temarel, 2009; Hirdaris et al., 2014; Hosseinzadeh et al., 2023). To accurately estimate the ship's hydrodynamic behaviour and powering requirement in waves, a key aspect is to understand the physics of complex interaction occurring at the stern of a ship between its propulsors, manoeuvring devices and the wake flow (Zhang et al., 2021). The hull's cross-sectional shape influences the fluid flow entering the propeller and rudder while the rotating propeller modifies the fluid flow around both the upstream hull and the downstream rudder. Likewise, the downstream rudder alters the upstream flow towards the propeller, impacting the thrust and torque it generates and also influences the pressure distribution and hydrodynamic forces and moments along the hull (Molland and Turnock, 2011; Badoe, 2015; Zhang et al., 2024).

* Corresponding author at: Maritime Engineering, University of Southampton, Boldrewood Campus, Southampton, SO16 7QF, Hampshire, UK.
E-mail addresses: s.hosseinzadeh@soton.ac.uk (S. Hosseinzadeh), Yifu.Zhang@soton.ac.uk (Y. Zhang).

https://doi.org/10.1016/j.oceaneng.2024.119258
Received 2 July 2024; Received in revised form 30 August 2024; Accepted 12 September 2024
Available online 19 September 2024

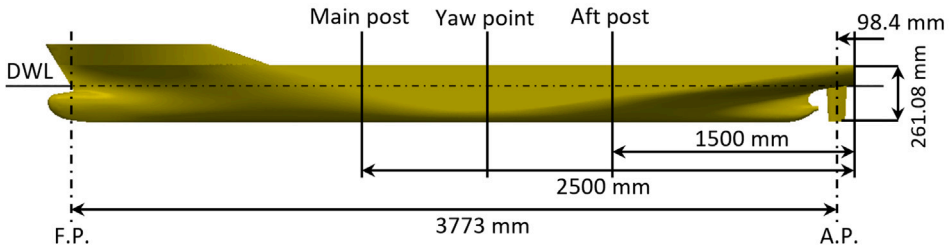

(a) A schematic view of test setup with the location of measurement points

(b) KCS rudder view from the stern of the model

(c) KP505 propeller model

Fig. 1. Experimental setup for KCS model: hull, rudder and propeller.

In the lee of the ship, where the fluid flow is shielded from direct wave action, the pressure typically drops due to the acceleration of the fluid around the ship's stern. This effect is further compounded by the presence of the propeller, which imparts additional momentum to the fluid, causing it to accelerate and change direction. Such dynamics can lead to varied flow patterns that significantly impact the rudder's effectiveness and, consequently, the ship's overall propulsive efficiency (Zhang, 2023). Furthermore, waves introduce additional forces and motions including added mass forces, damping forces and motions of heaving, pitching and rolling and these significantly complicate the fluid dynamics around the hull and its appendages. Waves are not generally uniform and can vary greatly in height, length, direction, and frequency (Temarel et al., 2016). They may manifest as swells or randomly generated waves, which should be analysed through the wave spectrum. This analysis includes considerations of wave spectrum bandwidth and wave–wave interactions. The specific characteristics of waves depend on the ocean or sea where the ship operates. In tropical zones, swells and narrow-band waves are more common, whereas in the North Atlantic and Southern Ocean, strong wind-generated waves are more frequently encountered. Consequently, the wave climate and the random nature of the wave itself also can be an important contributor. This variability makes it difficult to develop models that can accurately predict performance across all possible sea states (Tezdogan et al., 2015).

Traditional ship design has typically concentrated on optimising performance at a single design speed under calm water conditions (Molland et al., 2017). This approach normally includes incorporating suitable power margins to account for dynamic effects. However, this method often falls short in addressing the complexities introduced by real-world conditions, such as varying wave patterns and variable courses during voyage. Benefiting from the rapid progress of computing and numerical simulation method, the use of Computational Fluid Dynamics (CFD) has become an integral part of the ship design process (Zhang et al., 2023). The benefits of using CFD when considering some elements of the ship design is emphasised in the holistic ship design which was introduced in the last decade (Papanikolaou, 2010), and it considers all aspects of the ship, especially its hydrodynamics. The CFD can offer detailed insights into the local flow field, particularly regarding hull-appendage interactions in the stern region under various operating conditions, including calm water and waves (Zhang, 2023). Lee et al. (2008) conducted a numerical analysis to examine the flow characteristics and pressure distribution around a rudder device positioned in the wake of a propeller and hull of a low-speed, full-scale ship. Phillips et al. (2010) and Krasilnikov et al. (2011) investigated the propeller-rudder interaction, including the flow field and rudder performance, by simulating the flow around a fully appended ship model. This approach provided a more comprehensive understanding of the interaction mechanism using CFD. Wang et al. (2018) utilised the in-house CFD solver naoe-FOAM-SJTU to directly simulate ship manoeuvring in waves with rotating propellers and turning rudders, delivering detailed local flow characteristics of the hull, propeller, and rudder. Yilmaz et al. (2020) demonstrated the effectiveness of a state-of-the-art commercial CFD code in investigating the propeller-rudder-hull interaction, particularly focusing on cavitation phenomena such as tip vortex cavitation (TVC). Woeste et al. (2022) studied the hull-propeller-rudder interaction in head sea conditions using both CFD and a hybrid CFD and potential flow method. Their findings revealed that hull-propeller interaction in waves, along with nonlinear hydrodynamic and viscous effects, play a significant role in added power, with the added power coefficient exhibiting a nonlinear dependence on the square of the wave elevation.

Although CFD methods offer valuable insights into hull-appendage interactions in real seaways, there is still a significant need for detailed experimental validation data. This data is crucial for accurately

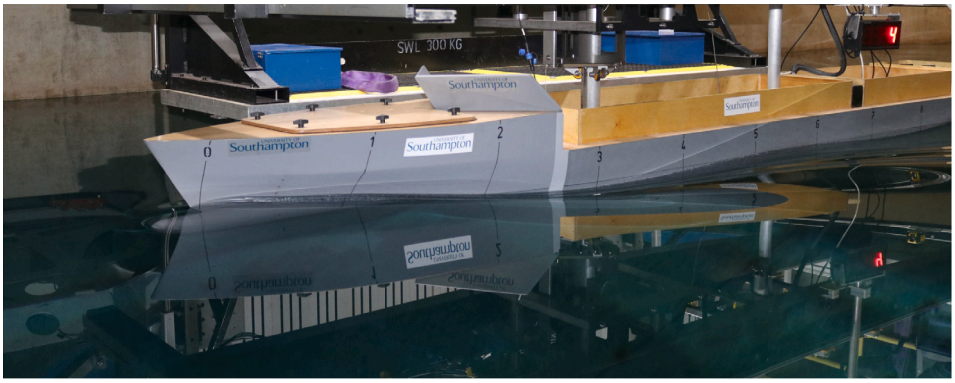

(a) Calm water resistance test with the model attached to the carriage

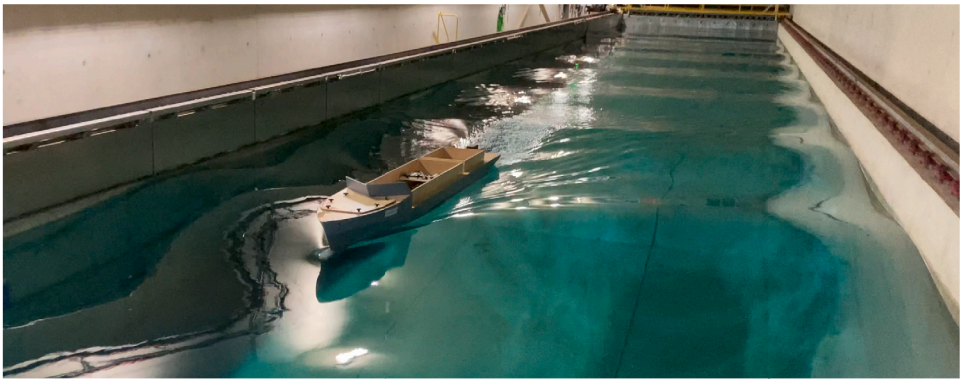

(b) Free running test with the wave in following sea condition

Fig. 2. A view of the UoS KCS model in the Boldrewood towing tank.

predicting hull-propeller-rudder interactions and the dynamic performance of a manoeuvring ship in waves. Experimental data also offers insights into the actual physics of scenarios. Virtual tests run with CFD codes are inherently constrained by certain assumptions and equations, physical tank tests, despite being limited by factors such as scale or depth, provide us with real data. This enables a deeper and more accurate understanding of the underlying physical phenomena. Furthermore, experimental data serves as benchmarks for calibrating and improving CFD simulations, leading to enhanced predictive capabilities. The progress of ship hydrodynamics in calm water and waves using experiments has been summarised in Gorski (2002), Stern et al. (2011), Larsson et al. (2013) and Hino et al. (2020). More recently, Tacar et al. (2020) experimentally studied the performance of a novel energy-saving device, Gate Rudder® (GR) system and found GR significantly reduced the power requirement of a ship, leading to higher ship propulsive efficiency. Sanada et al. (2021) conducted experimental study of hull–propeller–rudder interaction for steady turning circles of KCS with the aim at providing a physical explanation for the differences between the port and starboard turning circles. Köksal et al. (2022) conducted towing tank tests to measure resistance, propulsion, and seakeeping performance using a scaled model of the GATERS target ship and the aim was to establish the best procedure for estimating the powering prediction of a ship retrofitted with a GRS in both calm water and waves, utilising experimental methods. Although progress is made in experimental approaches, conventional tank testing mainly focuses on towing a scale ship model at zero drift, just allowing it to heave and pitch freely and most tests are conducted in calm water conditions (Zhang et al., 2022), with more advanced analyses performed in regular head waves and, when possible, following waves. During these tests, forces and moments are measured, with added resistance calculated as the difference between calm water and wave conditions (Bowker et al., 2023). However, these kinds of tests are insufficient to study the unsteady dynamic performance of a free running ship model navigating through irregular waves with non-zero drift angles. Therefore, to gain a deeper understanding of hull-propeller-rudder interactions and to provide high-quality data for CFD validation, synchronised time-accurate data is essential. This includes measurements of wave height, ship motion, hull forces, propeller RPM, thrust and torque, and rudder forces and moments.

This paper presents a detailed overview of the newly built geosim for the fully appended benchmark vessel, the Korean Container Ship (KCS). This advanced, highly instrumented self-propelled model is designed to accurately capture the vessel's time-accurate hydrodynamic performance in both towed and free-running conditions. Furthermore, this study encompasses the test program conducted for this ship model, detailing the data collected across four distinct testing campaigns. This research is driven by the need to enhance understanding of ship hydrodynamics in varied wave conditions using a free-running model scale ship. Despite extensive studies in this field, gaps remain in comprehensively assessing how different waves (both regular and irregular waves), drift angles and propeller thrusting loadings influence the hull-propeller-rudder interaction and overall ship powering performance in real sea states. This study aims to bridge this knowledge gap by systematically investigating the hydrodynamic responses of ships under these conditions. The experimental data collected from tests in both regular and irregular waves can provide new insights into the validation and verification of CFD simulations of 6 DOF (degree of freedom) ship manoeuvring in waves. The remainder of this paper is organised as follows. The experimental setup in this study is outlined in Section 2. Section 3 provides a detailed data processing. Results and discussion are detailed in Section 4. The paper concludes in Section 5 with a summary of the key findings and implications of the research.

Table 1
Principal dimensions of instrumented KCS model.

Parameter	Unit	Full scale	UoS model
Scale (λ)	–	1	60.96
Displacement (Δ)	tonne	52 030	0.23
Depth (D)	m	19.0	0.312
Breadth (B)	m	32.2	0.528
LPP (L_{PP})	m	230	3.773
LWL (L_{wl})	m	232.5	3.814
Draft Amidships (d)	m	10.8	0.177
KCS Rudder	NACA 0018	NACA 0018	
Wetted Area Rudder ($W_{SA} - Rudder$)	m^2	115	0.031
Wetted Surface Area (W_{SA})	m^2	9539	2.567
Propeller	KP505 (NACA 66) 5 blade	KP505 (NACA 66) 5 blade	
Propeller Diameter (D_p)	m	7.9	0.13
Ae/Ao	0.8	0.8	
Propeller rotation direction (from stern)	Clockwise	Clockwise	

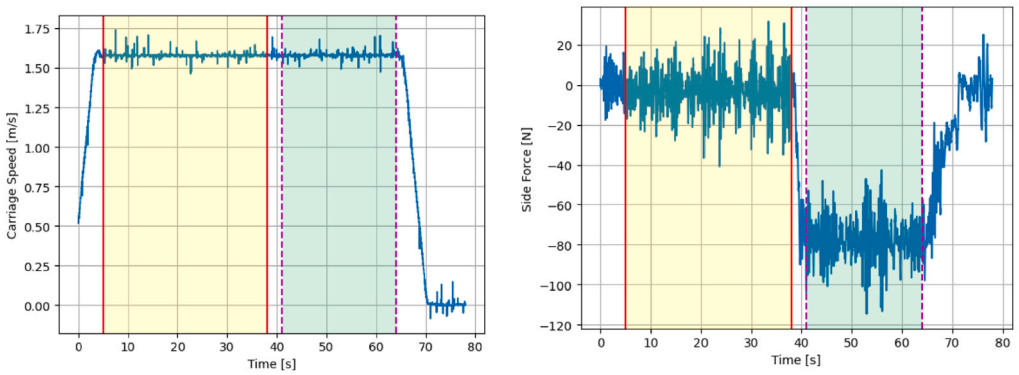

(a) (b)

Fig. 3. Plots taken from a specific run showing identification of two phases of a single test corresponding to rudder angles of 0 and 20 deg. Both sets of data are raw e.g., unfiltered.

2. Experimental setup

All experimental campaigns discussed in this paper were conducted at the University of Southampton's Boldrewood towing tank. This facility, which became fully operational in February 2022, measures 138 m in length, 6 m in width, and 3.5 m in depth, and it features a maximum carriage speed of 10 m/s (Malas et al., 2024). At the western extremity, the tank is equipped with twelve independent 0.5 m HR Wallingford wave generators, while the eastern end contains a passive beach. Additionally, a deployable side beach runs the full length of the southern wall. The carriage drive system is designed to facilitate testing at up to four different towing speeds per run. A fixed RPM controller can be set to predefined, and similarly, rudder angles can be preset. This setup enables efficient utilisation of each testing session, maximising the productivity and precision of the experiments conducted.

The synchronised measurements of motion, as well as propeller, hull, and rudder forces, effectively demonstrate the necessity of designing the propeller-rudder unit as an integrated system. Variations in propeller operating conditions are significantly influenced by rudder angle, ship orientation, and wave phase. Results from the four test campaigns exemplify the profound understanding and the level of uncertainty analysis required for validating numerical models. These findings could be considered as a benchmark for best practices in experimental testing. The initial phase of model development confirms the capability for precise measurements, which is crucial before embarking on long-duration tests similar to those previously conducted with an earlier tanker model (Bassam et al., 2019).

2.1. Model description

As part of the UK's Clean Maritime Demonstration Project Programme (AMPS-USV), a newly constructed scaled model of the KCS hull (Hino et al., 2020) was equipped with various advanced instruments. These included load cells for measuring propeller thrust and torque, an RPM encoder, a three-component rudder dynamometer, and a six-degree-of-freedom inertial measurement unit. A geosim model of the KCS hull form at a scale of 1:60.96, hereafter referred to as the UoS model, was constructed using laser-cut plywood frames and strip planks and finished with a hydrodynamically smooth paint coating. The specific dimensions of the model are detailed in Table 1. This model features a detachable bow, allowing for the attachment and testing of various bow designs. Standard trip studs are mounted at 5% of the model's length from the bow. The model was towed using a twin-post system, which employed a manufactured plate fitted into the model. The main post was positioned 2.5 m from the stern, while the secondary post was 1.5 m from the stern. The yaw pivot point, which establishes the drift angle, was located 2.0 m from the stern, centred between the main and secondary posts. The rudder dynamometer was installed 98.43 mm from the stern and 261.08 mm from the bottom of the model (Fig. 1(a)). This setup allows for a range of drift angles to be set between ±8 degrees in 0.5-degree increments. During drift tests, the twin posts are mounted along the towing tank centreline, constraining the model's motion to heave and pitch around the tank centreline rather than the ship axis system. Both the rudder and propeller were utilised in this experiment to provide valuable insights into the interaction between the hull, propeller, and rudder. A high-quality titanium alloy KP505 propeller was manufactured and used in the self-propelled tests, as detailed in Table 1 and depicted in Fig. 1(c). Additionally, a single-piece all-movable rudder with the same planform as the original semi-balanced skeg rudder was used for these experiments. The locations of the two posts, along with the model appendages including the rudder and propeller, are illustrated in Figs. 1(a) and 1(b).

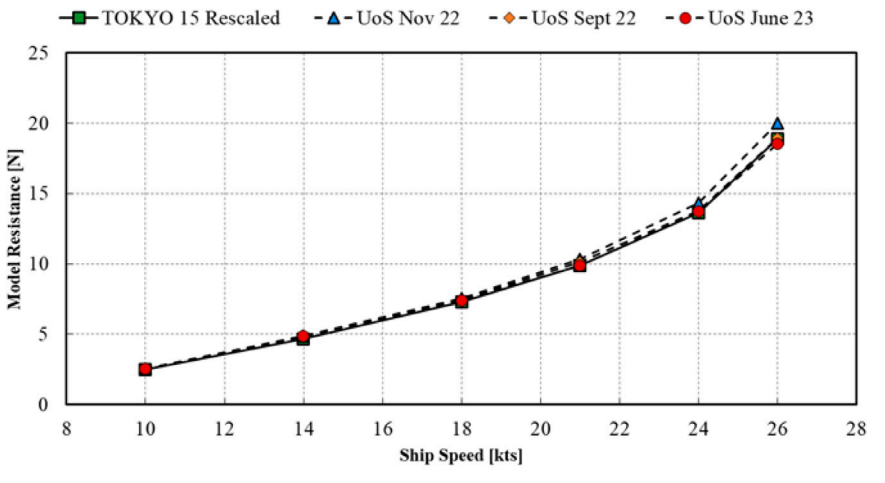

Fig. 4. The model calm water resistance comparison corrected to water at 15 °C (Hosseinzadeh et al., 2024b).

As the model was designed to work both when attached to a carriage and in a free running mode, it incorporated its own power and control systems. Power was supplied by two sets of appropriately sized lithium-ion batteries, providing up to eight hours of operation. This capability ensures a full day of testing, either in the towing tank or in an open water environment such as a lake or basin. A reaction torque load cell attached to the electric motor casing facilitates precise measurement of propeller torque in real-time. The motor is mounted on a sliding system, enabling the measurement of propeller thrust. An optical sensor is employed to measure the RPM. The propeller's RPM can be set and maintained at a constant level using a proportional controller, which is operated via a modified radio control unit. For directional control during free running operations, a suitable rudder controller was required. This was achieved with a radio control unit capable of fixing a calibrated rudder angle or varying it as needed. The system is designed with future upgrades in mind, allowing for the potential implementation of fully autonomous operation.

2.2. Test procedure

A consistent procedure was adhered to across all test programmes. Initially, the model was ballasted to its design draft (d = 0.177 m), with slight variations in ballast locations required based on the specific instrumentation systems utilised. For example, drift angle tests necessitated the use of an attachment plate. The tests typically spanned tank bookings of two to five days, conducted in February, March, September, and November 2022, as well as the most recent in June 2023. Representative results from these test campaigns are included in this report. After each series of tests, the systems were further refined, with the most significant improvement being the first utilisation of the rudder dynamometer in June 2023. Figs. 2(a) and 2(b) depict views of the model during the conventional test attached to the carriage and the free running test, respectively.

The development of the test programme for this model captured relevant data from four distinct campaigns:

- Comparison tests with KCS benchmark geosim calm water resistance data (February 2022), presented in Section 4.1.
- Experimental uncertainty of time-accurate data from laboratory tests of the SESS6077 Zero Carbon Ship Resistance and Propulsion master's module (November 2022), presented in Section 3.
- Performance in waves for both towed and free-running modes (March and September 2022), presented in Section 4.2.

Table 2
Details of regular wave properties.

Parameter	Wave-1	Wave-2
λ/L_{PP}	0.651	1.150
Wavelength (m)	2.455	4.338
Wave period (s)	1.254	1.667
Phase speed (m/s) – (c_p)	1.958	2.602
Wave group speed (m/s) – (c_g)	0.979	1.303
Wave amplitude (m)	0.019	0.038
Wave steepness (–)	0.0486	0.055

- Interaction effects of a towed model at drift angles, with and without waves (September 2022 and June 2023), presented in Section 4.3. The raw data from this series of experiments are available in Hosseinzadeh et al. (2024a)

Furthermore, Table 2 illustrates two distinct head sea regular waves utilised in the experiments. These specific wave frequencies were chosen to comprehensively investigate the effects of different sea states on hydrodynamic interactions. This table provides the details of each wave, which will later be used to normalise the measured results. The effect of waves on the model's performance when towed at a steady angle of drift was investigated, and the details of these experiments are presented in Table 3.

2.3. Data acquisition

The requirement for high-resolution, time-accurate data necessitated the selection of a 250 Hz data acquisition rate. Three distinct systems were employed in these experimental campaigns. The first is an onboard system capable of capturing data from 16 channels, offering flexibility in selecting data sources. Data acquisition (DAQ) for specific runs is managed by one of the onboard micro-PC (GPD MicroPC) systems via a remote desktop connection. Another micro-PC controls the data acquisition from a nine-degree-of-freedom inertial measurement unit (IMU). This IMU measures translational and rotational accelerations, as well as orientation, utilising a magnetometer. The towing tank dynamometer, designed and manufactured by the University of Southampton's Wolfson Unit for Marine Technology and Industrial Aerodynamics (WUMTIA), is capable of measuring six components of force and moment. For the purposes of these tests, the focus is on drag, side-force, and yaw moment. To accommodate the use of two posts, an additional force block was installed at the base of the guide-post. This block is engineered to measure side-force and present

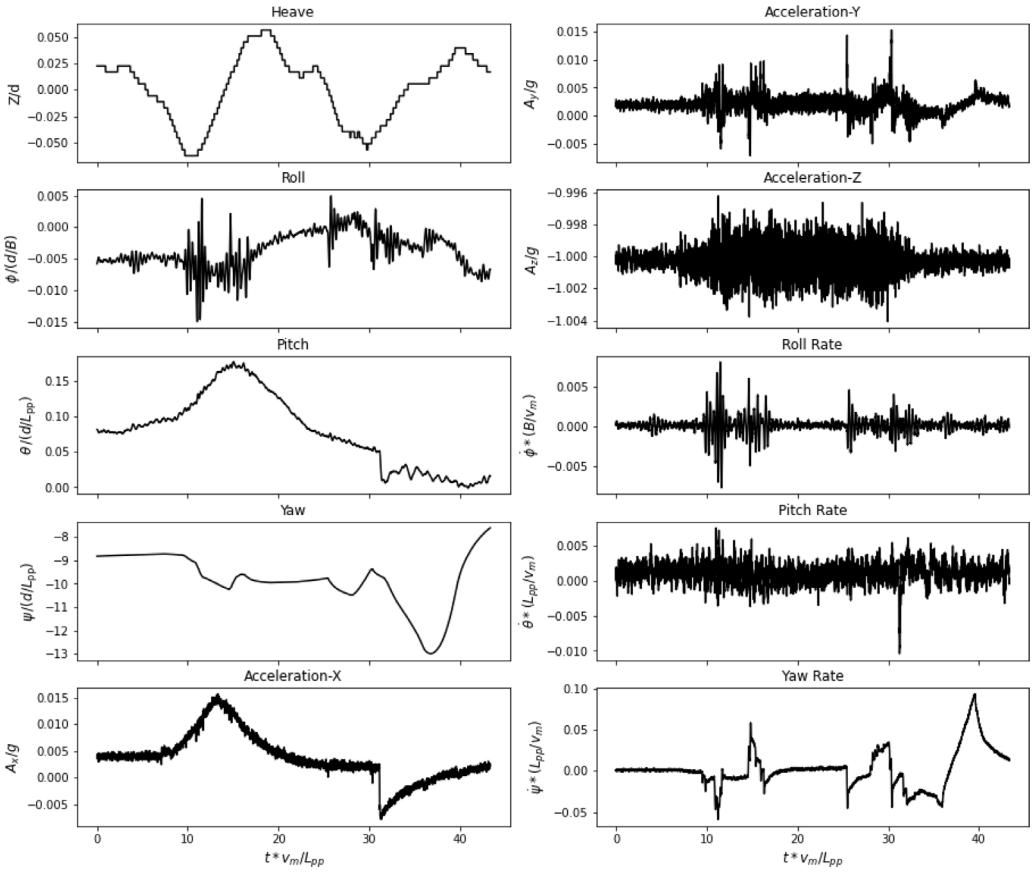

Fig. 5. IMU data showing heave, pitch and yaw (course along tank), three translational accelerations, and three angular rates for calm water (The propulsion system measurements of this run are presented in Fig. 6).

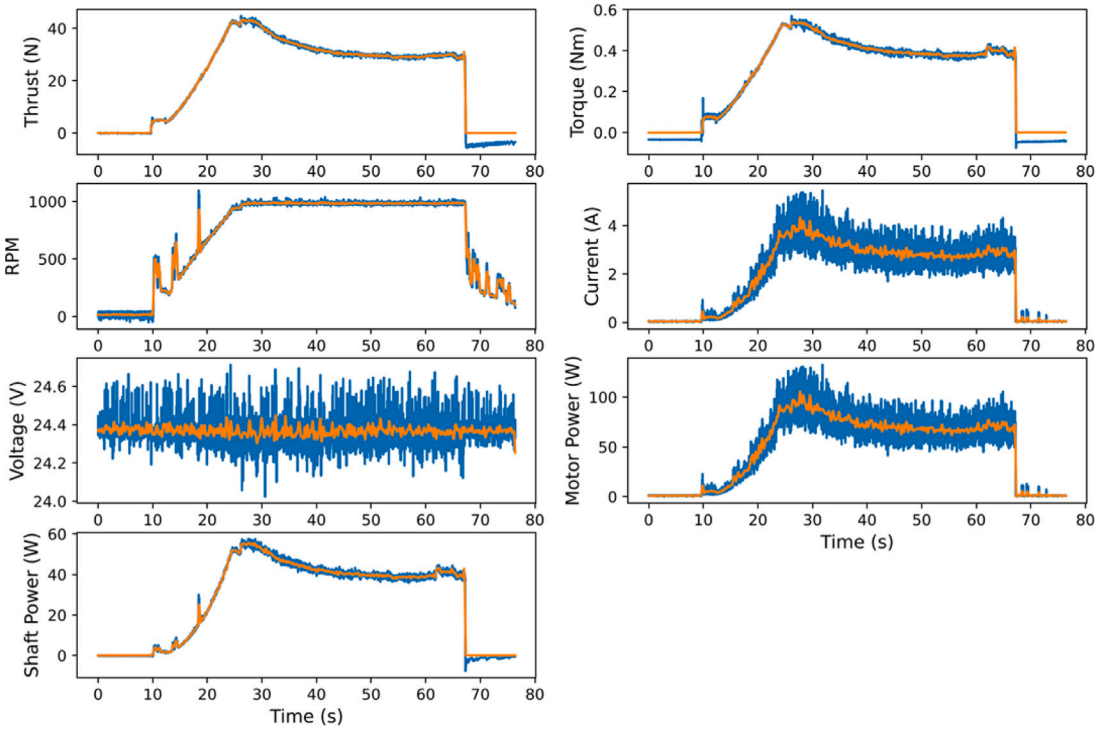

Fig. 6. LASSO data for onboard propeller and power: Constant speed is maintained from 50 s onwards. Spikes on the RPM are attributed to occasional optical system dropouts rather than actual changes in RPM (related to Fig. 5).

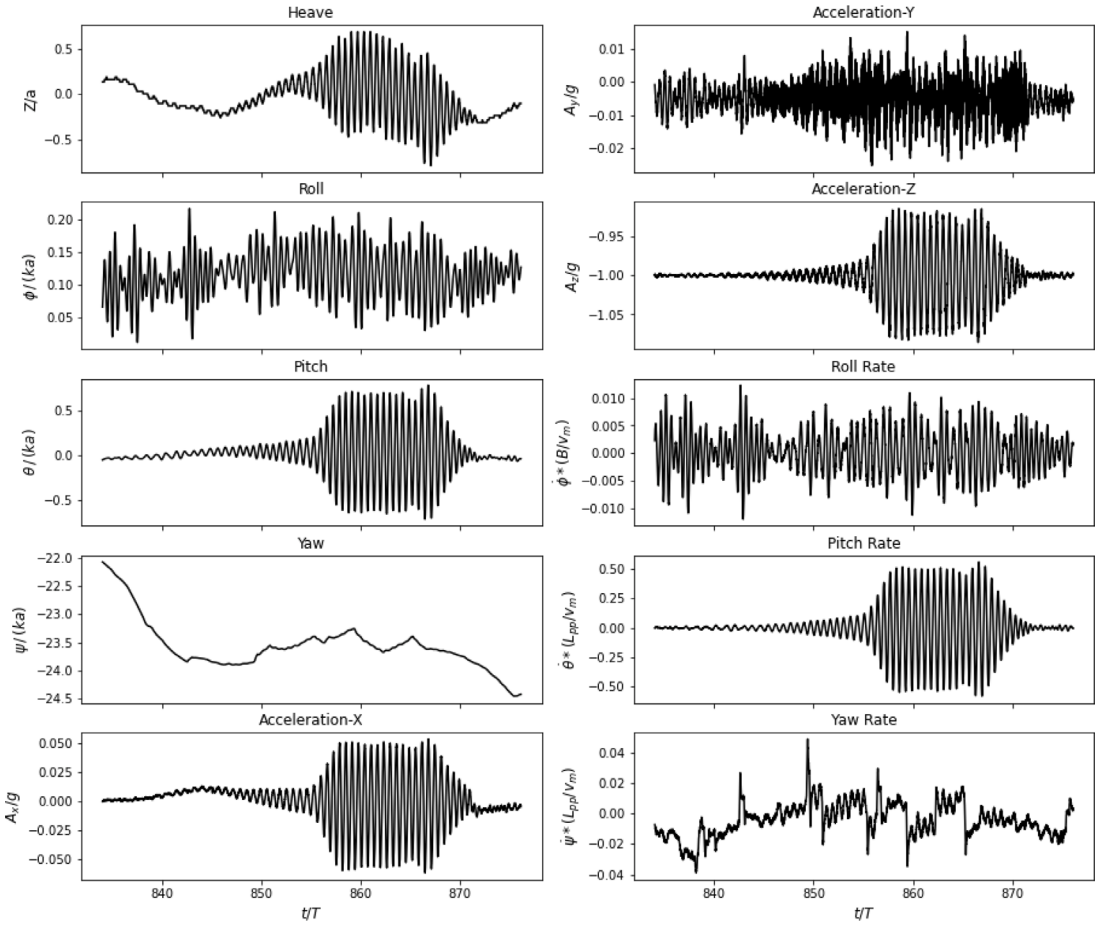

Fig. 7. IMU data illustrating how ship motions vary with sea state at a constant RPM (Fig. 9): Regular head sea (Wave-2 in Table 2) with wave amplitude $a = 0.038$ m, and wave period $T = 1.66$ s.

no resistance in the drag direction. Further information, including the laser-based system used to measure carriage position and speed, can be found in Malas et al. (2024) and Hosseinzadeh et al. (2024b). The setup also includes heave and pitch sensors, along with a wave elevation ultrasonic sensor mounted near the front of the carriage, positioned at one-third of its width. The data acquisition system on the carriage supports 16 channels and records the position and speed of the carriage. Due to the low force levels anticipated on the rudder, a specialised Force-Torque sensor from ATI Industrial Automation was procured. The dynamometer is mounted on the deck in a waterproof housing and connected to the rudder via a shaft. A servo controller and angle position sensor, operated through a radio control unit, enable remote setting of the rudder angle. Typically, it was possible to measure three or four rudder angles per run during the tests. A supplied calibration and interaction matrix allows measurement of six components, with particular interest in the side-force, drag, and yaw moment. Additionally, the x and y axis moments help determine the spanwise centre of pressure. Synchronising the acquisition of data from complementary DAQ systems presents a challenge. When the model is attached to the carriage, the onboard and carriage systems can be synchronised by splitting a cable to acquire the same signal on both systems. Synchronising with the IMU is more complex but can be inferred from the x-axis acceleration and propeller measurements. Changes in rudder angle, when not directly measured, can be deduced by observing variations in the side-force on both the rudder dynamometer and hull side-force channels. The wave elevation data provides details on the onset wave conditions, which are programmed from the carriage. Tests have been conducted in both head and following seas. For head seas, a wave system is generated and progresses along the tank. As the wave train approaches the beach end, either the carriage motion begins, or the free running model is accelerated to the test speed. For free-running tests, calibration runs were performed to determine the average model speed, ensuring that the carriage and model maintained the same relative position. It was observed that the model operator could keep a consistent track along the tank centreline, with deviations in lateral acceleration recorded by the IMU. This series of experiments was conducted following the recommendations of the International Towing Tank Conference (ITTC) (ITTC, 2008, 2011, 2017) and the guidelines for self-propulsion tests outlined in Bassam et al. (2019).

3. Data analysis

Typically, up to three data files were recorded per test run: onboard (LASSO), carriage (NI), and motion (IMU). Since data was collected over the entire length of the carriage or model run, the initial phase of analysis involves segmenting the data into specific test segments. The carriage controller allows for up to four different speeds during the model's progression down the tank, with potential variations including changes in propeller RPM or rudder angle. Data points corresponding to transitions in speed, RPM, or angle are excluded from the analysis. Additionally, the initial start and finish phases, when the model is at rest, can provide useful checks for 'zero' load conditions. Given that the educational purposes of the instrumented model, automatic data acquisition was not employed. Instead, a basic toolkit of Python routines and an associated Jupyter Notebook environment were used. This setup enables the investigation of various filters and processing techniques on the data, providing a deeper understanding of data quality and measurement errors. Python scripts facilitate automated processing

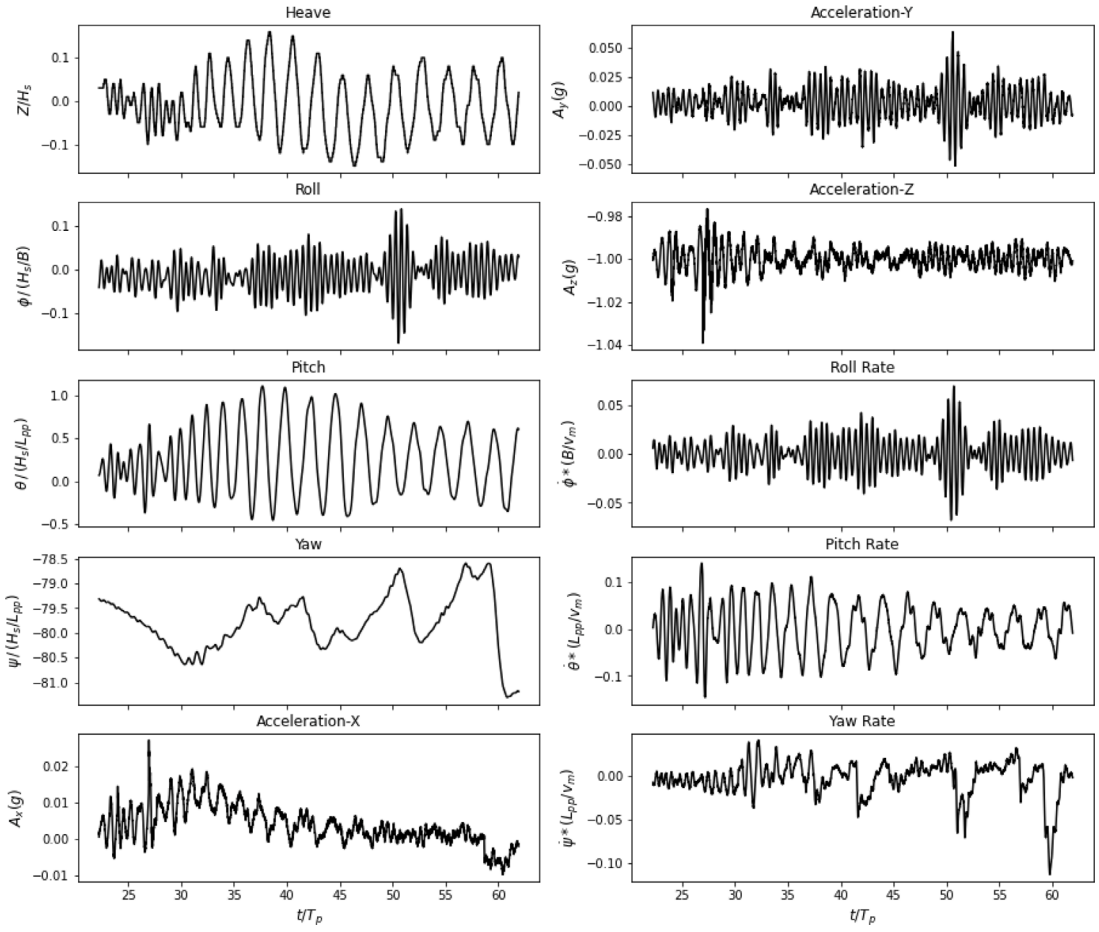

Fig. 8. IMU data illustrating how motions vary with sea state at a constant RPM (Fig. 10): Irregular following sea with the significant wave height of $H_s = 0.1$ m and the wave peak period of $T_p = 1.66$ s.

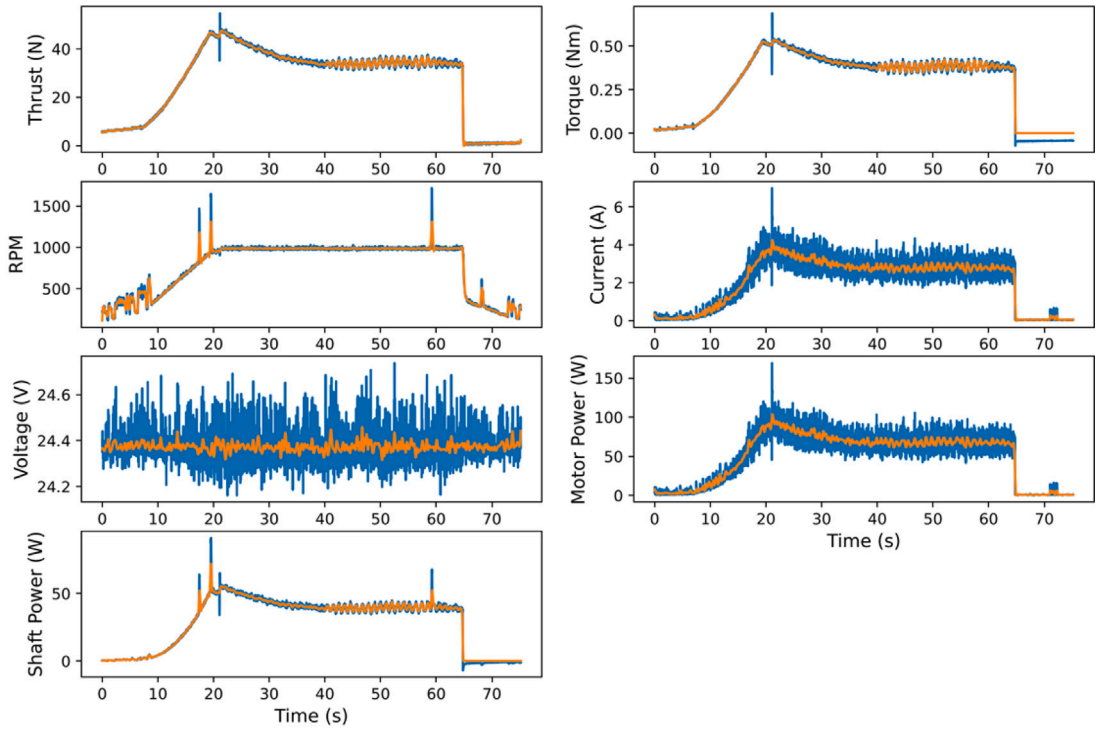

Fig. 9. LASSO data showing power variation with sea state at a constant RPM: Regular head sea (related to Fig. 7).

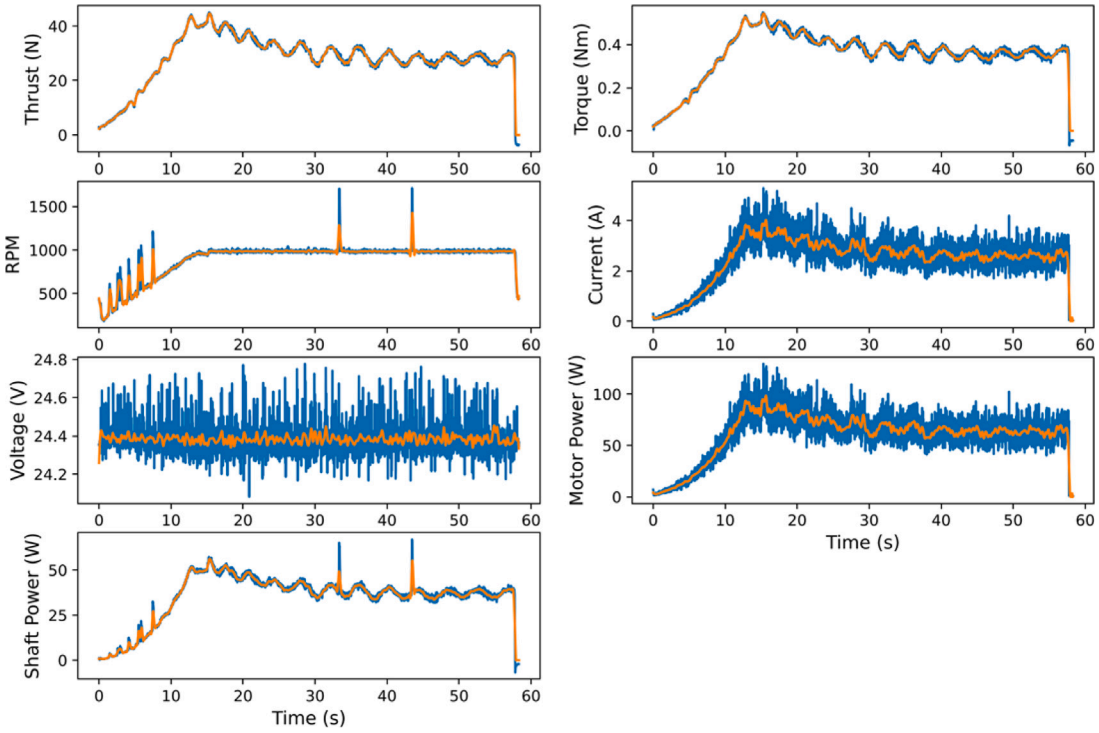

Fig. 10. LASSO data showing power variation with sea state at a constant RPM: Irregular following sea (related to Fig. 8).

and comparative data presentation. Unlike conventional acquisition systems, which typically record data only under steady conditions, this method offers a more comprehensive view of the data. The data acquired has implicit filtering from the 250 Hz acquisition rate and analogue-to-digital conversion. Once the run segments are identified by their start and finish times, the frequency content of the signal provides significant insights into the behaviour of the dynamometer system. The objective of the KCS Powering Laboratory within the SESS6077 Zero Carbon Ship Resistance and Propulsion module was to examine the impact of signal processing and other sources of uncertainty on the experimental determination of ship powering performance during a test run. To achieve this, a series of tests were conducted, including:

- Baseline calm water resistance tests with the rudder set at either zero or 20 degrees.
- Self-propulsion tests at speeds close to design, varying RPMs and rudder angles of 0 and 20 degrees.
- Self-propulsion tests at speeds close to design in regular waves, with rudder angles of 0 and 20 degrees.
- Self-propulsion tests at speeds close to design in irregular waves, with rudder angles of 0 and 20 degrees.

Figs. 3(a) and 3(b) demonstrate how the run segments were divided to accommodate changes in rudder angle in carriage speed and side force measurements, respectively. During these tests, the propeller operated at 956 RPM, and the model was tested in waves with a frequency of 0.798 Hz, amplitude of 0.019 m (Wave-1 in Table 2), and a carriage speed of 1.58 m/s.

Table 4 presents the calculated mean, variance, and uncertainty for the carriage measurements. The significant variability is primarily attributed to wave-induced movements, impacting thrust, torque, and drag under wave conditions. Table 5 displays the uncertainties corresponding to the dimensionless parameters.

4. Results and discussions

4.1. Resistance in calm water

The KCS hull was selected for development in the Boldrewood towing tank to facilitate comparisons with decades of test results, particularly from ITTC-inspired CFD validation workshops (Hino et al., 2020). To assess experimental accuracy, model resistance measurements in calm water are compared with previous tank experiments and the TOKYO'15 data (Hino et al., 2020). These tests, conducted with zero leeway angle, zero rudder angle, and no propeller, represented the calm water data for the bare hull with rudder appendage. Table 6 details the total resistance of the model (R_{TM15}) at 15 °C and the differences from the TOKYO'15 data, with 'V_S' indicating the speed of the full-scale ship, 'V_m' the speed of the scaled model, and 'F_n' is the Froude number. The largest discrepancies were attributed to some uncertainty in the precision of the ballasting during the student laboratories in November 2022. Fig. 4 compares the resistance values in calm water for the three most recent tests with a scaled dataset from the Tokyo 2015 CFD workshop (Hino et al., 2020), demonstrating the consistency and reliability of the Boldrewood towing tank results and underscoring the KCS hull's suitability for ongoing experimental and CFD studies.

4.2. Powering performance in waves

The powering trials with the scaled model were conducted as part of the study to explore how ship motions might affect the performance of fuel cells used for ship propulsion. This involved a series of tests in various regular and irregular sea states, both in head and following seas. While some initial tests were towed, the primary focus was on free-running tests, with the RPM set to achieve an average model speed of 1.58 m/s, corresponding to the design speed. The speed was verified using the encounter frequency. The performance of the instrumented model under three example conditions is presented. Figs. 5 and 6 depict the self-propelled condition in calm water from the same run, serving as a benchmark for the IMU and onboard (LASSO) data, respectively. The

Table 3
KCS at drift in waves test matrix.

Model speed	Drift angle	Rudder angle	Wave frequency	Wave amplitude	Propeller RPM
Vm = 1.581 m/s (Fn = 0.26)	−5°	−10°	0.798 Hz	0.019 m	RPM_1 (n = 10.0)
	0°	0°			
	2.5°	10°	0.600 Hz	0.038 m	RPM_2 (n = 18.3)
	5°	20°			
	7.5°				

Table 4
Mean values and Type A uncertainties for measurements.

Parameter	Run number	Arithmetic mean	Variance	Standard uncertainty
Water temperature [degrees]	Run 1 and 2	17.4	0.798	0.0304
Propeller thrust [N]	Run 1	16.691	0.13314	0.006362
	Run 2	17.338	0.14998	0.39981
Propeller torque [N]	Run 1	0.343	8.80E−05	0.000164
	Run 2	0.352	9.98E−05	0.000207
RPM	Run 1	955.872	751.751	0.478085
	Run 2	956.7	608.146	0.511768
Carriage speed [m/s]	Run 1	1.578	7.499	0.000151
	Run 2	1.58	7.737	0.000183
Drag [N]	Run 1	0.77	453	0.371
	Run 2	1.393	371.2	0.3998
Side force [N]	Run 1	−3.252	104.4	0.1782
	Run 2	−77.769	101	0.2085
Heave [mm]	Run 1	−7.777	2.3	0.02645
	Run 2	−7.675	3.057	0.03628
Trim [mm]	Run 1	0.666	0.373	0.0107
	Run 2	0.43	0.336	0.012

Table 5
Non-dimensional parameter uncertainties. Note: these are high because the response of the ship is periodic with the wave field encountered.

	K_T	K_Q	Re	Fn	C_T	C_L
Run 1	0.231	0.0364	5 555 000	0.2582	0.00554	0.0
Run 2	0.239	0.0373	5 562 000	0.2586	0.00593	0.0236
Type	Type A	Type A	Type A	Type A	Type A	Type A
Standard uncertainty (Run 1)	0.6761	0.6761	0.000151	0.000151	0.371	0.000214
Standard uncertainty (Run 2)	0.8268	0.7237	0.000183	0.000183	0.3998	0.000258

Table 6
Comparison of model total resistance to TOKYO'15 data at 15 °C water temperature and in calm water condition (Hino et al., 2020; Hosseinzadeh et al., 2024b).

V_S	V_m	F_n	R_{TM15} (N)				Comparison to Tokyo 15 data (%)		
(knots)	(m/s)		TOKYO 15	Sept 22	Nov 22	June 23	Sept 22 (ΔR_T)	Nov 22 (ΔR_T)	June 23 (ΔR_T)
10.00	0.659	0.11	2.49	2.51	2.56	2.56	0.84	2.56	2.75
14.00	0.922	0.15	4.65	4.81	4.86	4.86	3.48	4.67	4.56
18.00	1.186	0.19	7.31	7.44	7.57	7.43	1.76	3.54	1.60
21.00	1.384	0.23	9.87	10.11	10.35	9.90	2.42	4.82	0.25
24.00	1.581	0.26	13.61	13.77	14.32	13.72	1.17	5.20	0.80
26.00	1.713	0.28	18.90	18.95	20.00	18.51	0.22	5.81	2.08

time signals can be synchronised by the start of the RPM, which occurs at 10 s on the LASSO and 20 s on the IMU. To filter out high-frequency noise in the LASSO data, a 150-point rolling average was applied.

Figs. 7, 8, 9, and 10 present IMU and LASSO data for regular and irregular sea states, respectively, with the same propeller RPM setting. As shown in each figure, these series of data have been non-dimensionalised to enable better comparison across different scenarios and to provide more generalised and broadly applicable results. The calm water case is normalised using the model's geometric properties, while the wave cases are normalised using the properties of the waves. Additionally, the accelerations are normalised using g ($g = 9.81\,m/s^2$). In these figures, ϕ, θ, and ψ represent the roll, pitch, and yaw motions of the model (in radians), respectively, and $\dot{\phi}$, $\dot{\theta}$, and $\dot{\psi}$ represent their angular rates. These datasets provide comprehensive information about the performance of the ship in regular and irregular wave conditions. For instance, the human operator's course-keeping performance is evident from the changes in yaw. In the regular sea state, the short wavelength relative to the model scale has only a limited effect on motion and power response. In contrast, the irregular following sea, with its spectrum of wavelengths, induces more significant motions and power fluctuations. Such fluctuations in power demand can lead to efficiency losses in the power supply system, whether using a fuel cell or, in this case, a battery. These experiments underscore the importance of understanding the interactions between sea state and power demand. They highlight the potential for improved propulsion control using advanced controllers capable of predicting sea state variations. The data obtained from these trials is invaluable for developing more efficient and responsive maritime power systems.

4.3. Influence of drift angle on rudder-propeller-interaction

In addition to the calm water resistance and free-running tests, the interaction between the hull, rudder, and propeller at various drift angles was studied (Lee, 2023). A comprehensive investigation was conducted on the influence of waves on the powering performance of the KCS when towed at a steady drift angle. The range of parameters

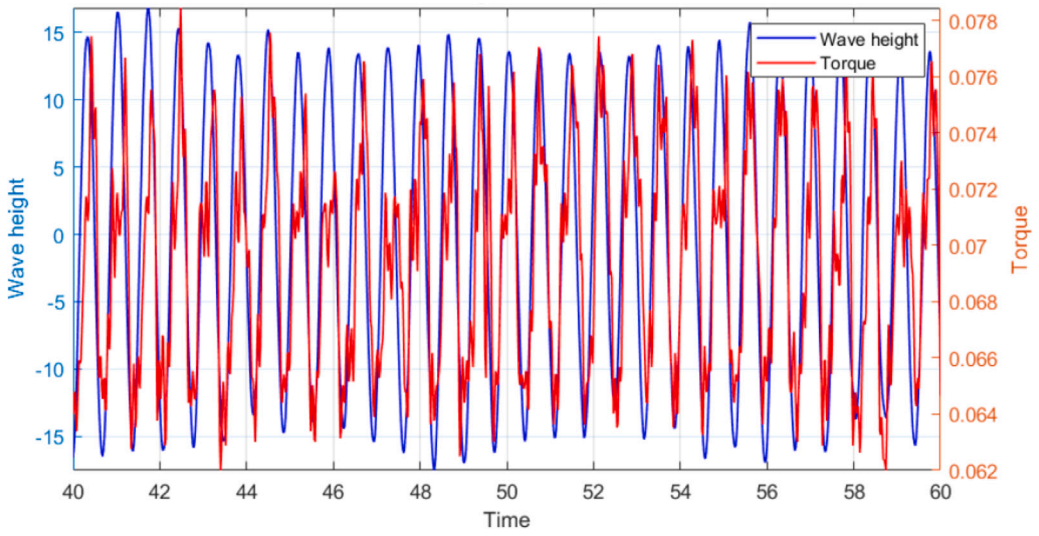

Fig. 11. Comparison of propeller torque for the test at constant rpm (RPM1) and the regular head wave of Wave-1 in Table 2 ($a = 0.019$ m and $T = 1.254$ s).

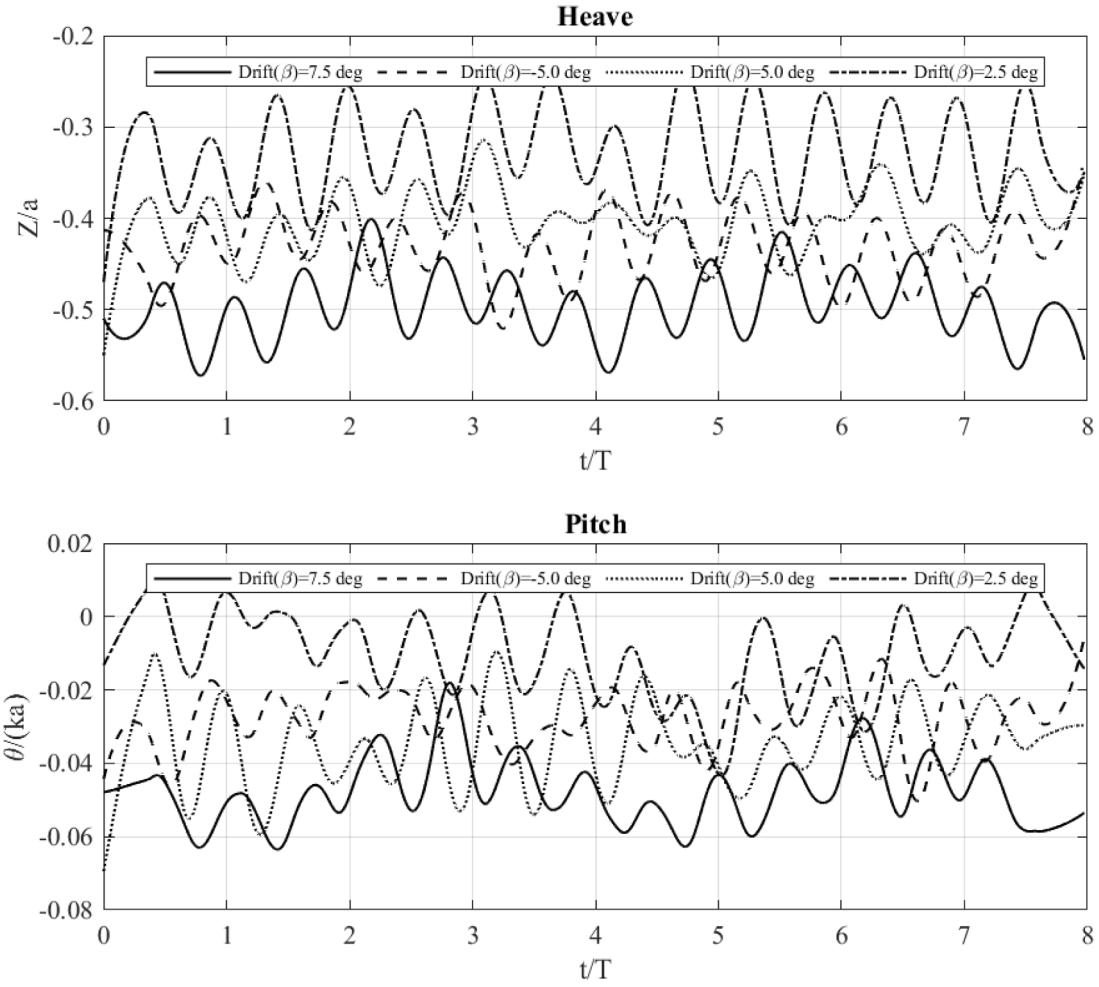

Fig. 12. Comparison of heave and pitch responses for a constant rudder angle ($\delta = 0$) for low amplitude wave (short wave: Wave-1) and four drift angles.

tested is detailed in Tables 2 and 3, with four rudder angles tested per run. All three data acquisition systems were employed in these tests, capturing a wealth of data, particularly regarding the periodic performance in waves. Fig. 11 illustrates the fluctuation of wave height and propeller torque over a series of regular wave encounters, highlighting the detailed nature of the data. As illustrated in this figure,

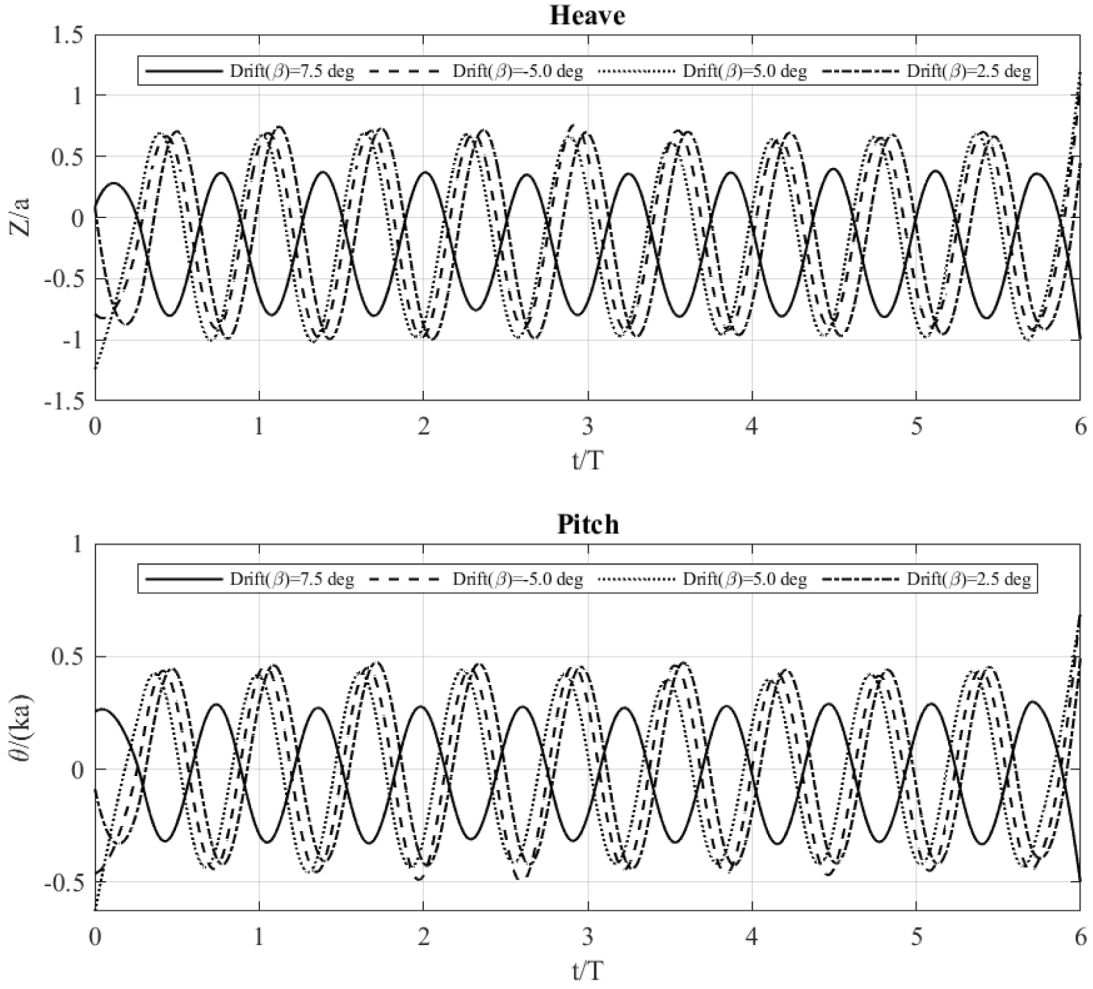

Fig. 13. Comparison of heave and pitch responses for a constant rudder angle ($\delta = 0$) for large amplitude wave (long wave: Wave-2) and four drift angles.

torque values are observed to vary in accordance with the wave cycle, closely following its periodic tendencies. These torque values align significantly with the properties of the wave. It should be noted that in the experimental configuration of this study, both pitch and heave were allowed to vary freely. This freedom in motion is likely a contributing factor to the observed correlation between torque values and wave cycles. Additionally, given that the effective wake conditions are not constant but fluctuate during wave conditions, the wave elevation at the plane of the propeller would also experience variations, further influencing the torque values.

Figs. 12 and 13 show the periodic variation in the model heave and pitch responses for different drift angles, with the model sitting deeper in the water at higher drift angles but exhibiting similar amplitude for all drift angles tested. In the case of wave-1, the ship's motion is relatively unaffected, demonstrating that the fluid forces exerted by this wave are minimal in comparison to the ship's size and mass. Interestingly, the data reveals that as the drift angle increases, the ship experiences greater submersion and a larger pitch angle, although the overall impact remains moderate. Alternatively, wave-2 has a pronounced effect on the ship's motion, causing it to mimic the wave cycle closely. This suggests that the fluid forces in wave-2 are substantial enough to significantly influence the ship's behaviour. The ship exhibits considerable pitch and heave motion in these conditions, which not only affects its overall stability but also has implications for the performance of its propulsion system, particularly the propellers. This, in turn, could have a substantial impact on the ship's speed. Similarly, it also shows that the ship experiences greater submersion as the drift angle increases. Furthermore, the observed differences in heave and pitch responses between short (wave-1) and long (wave-2) waves align with established principles in naval architecture. As expected, the short waves induce minimal vertical motion, while the longer waves result in more pronounced responses. This behaviour is consistent with typical response amplitude operator (RAO) plots for ships. It is worth noting that for ships in motion, additional factors come into play. Doppler effects change the apparent wave frequency experienced by the vessel, and a resonance zone typically emerges in longer wave regimes. In this resonance zone, the ship's response can be significantly amplified when the wave frequency approaches the natural frequency of the ship's motion. These phenomena collectively contribute to the complex dynamic behaviour of vessels in varying sea conditions.

Fig. 14 illustrates the impact of drift and rudder angle on the hull side-force coefficient (C_S) without propulsion and at two levels of self-propulsion (light and medium). The results are presented in the ship axis. These scenarios simulate conditions where a portion of the propulsive load comes from wind forces rather than the propeller. In non-self-propulsion conditions, the results indicate that the dimensionless side-force in calm water increases linearly with increasing drift angle, a trend consistent across different rudder angles. However, under self-propulsion conditions, the interaction between the rudder and the propeller leads to a greater force acting on the rudder. The larger the rudder angle, the greater the resulting moment and side-force on the ship. Examining the second and third plots, there is no significant effect at low RPM. However, at high RPM in the third plot,

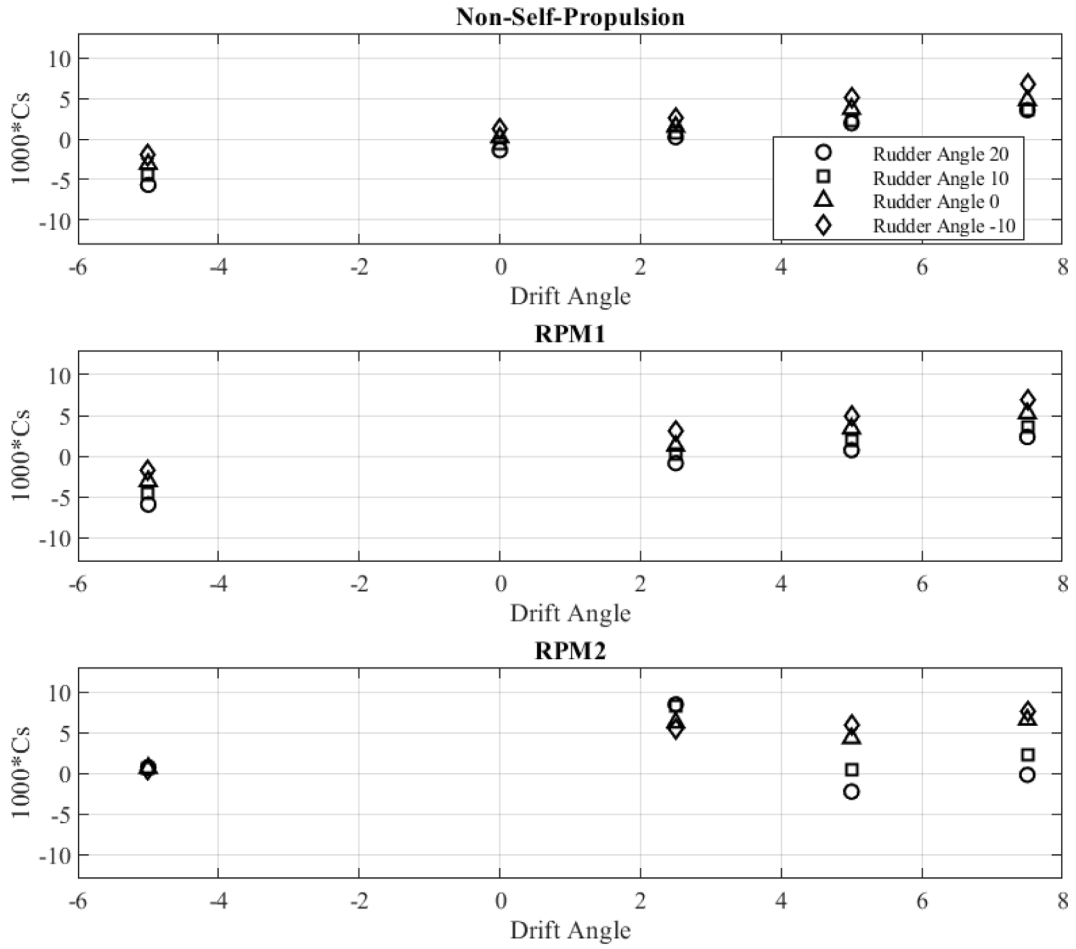

Fig. 14. Non-dimensional hull side-force for drift angles between −5 and +7.5 degrees and rudder angles between −10 and +20 degrees for towed model free to heave and pitch in calm water.

the side-force no longer follows a linear pattern and exhibits a different trend. This indicates the complex interaction between the propulsion system and the rudder at higher power levels. In addition, the side-force coefficient behaves quite differently in wave conditions. Figs. 15 and 16 show that as the drift angle increases, the influence of propeller speed and wave conditions becomes more pronounced. This variability should be particularly considered when designing wind-assisted ships, as their behaviour is expected to differ depending on their shape and sea conditions compared to regular ship shapes.

5. Conclusions

In this paper, a detailed overview of the newly built geosim for the fully appended benchmark ship model, the KCS hull is presented. It also provides an in-depth analysis of the test program executed for this model, including a comprehensive collection of data from four distinct testing campaigns.

According to the literature review presented in Section 1, although CFD methods offer critical insights into ship hydrodynamics in real sea states, there is a substantial demand for detailed experimental validation data to enable accurate prediction of hull-propeller-rudder interaction, thereby propulsive and powering performance in waves. This is particularly crucial for understanding the unsteady performance of manoeuvring ships in actual sea conditions. Experimental methodologies play a pivotal role not only in validating and verifying numerical models but also in serving as a benchmark for calibrating and enhancing CFD simulations. Such improvements are essential for advancing the predictive capabilities of these simulations. Furthermore, traditional towing tank tests primarily focus on evaluations in calm water conditions. For more advanced analyses, these tests may extend to a series of regular and, where feasible, following waves. In these scenarios, a scale model of a ship is towed at zero drift, allowing only for free heaving and pitching motions. However, these tests do not adequately capture the unsteady dynamic performance of a free-running ship model navigating through irregular waves at non-zero drift angles. Therefore, synchronised time-accurate experimental data is still in high demand for a better understanding of the mechanisms of hull-propeller-rudder interaction in waves.

The paper details the experimental setup in Section 2, which includes a concise overview of model description, test procedure and data acquisition. Section 3 presents the process of data analysis including experimental uncertainty and results and discussions of test programs conducted for the ship model is outlined in Section 4. The principal values and implications of this study are shown below:

- Employing an instrumented model greatly enhances the comprehension of resistance and powering data quality in experimental tests. This method facilitates more precise and detailed observations, contributing to assess ship hydrodynamic performance characteristics with greater accuracy. Nevertheless, the use of such sophisticated models incurs substantial costs. Specifically, depending on the required functionality and the size of the model being tested, the overall expenses associated with the model can increase by a factor of two to four. This cost escalation reflects the complexity and the advanced technology needed to equip and maintain these instrumented models for rigorous testing environments.

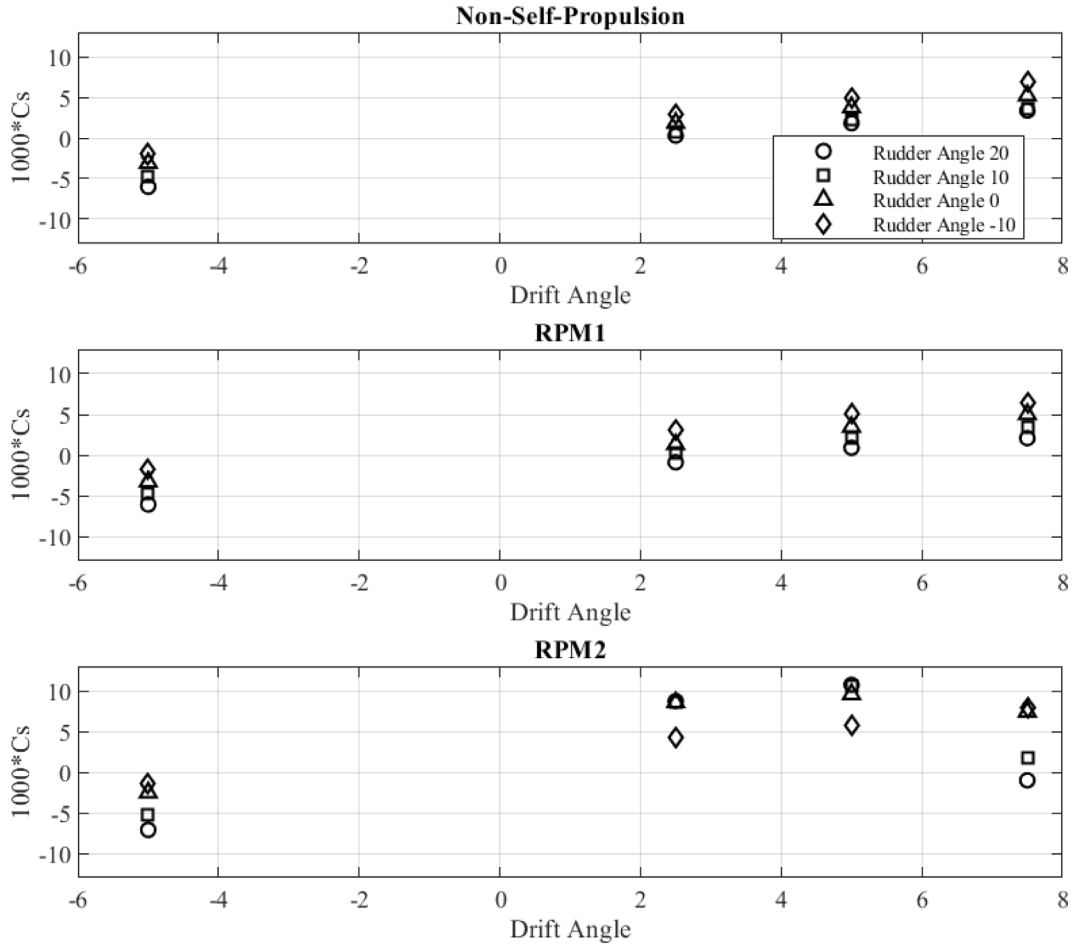

Fig. 15. Non-dimensional hull side-force for drift angles between −5 and +7.5 degrees and rudder angles between −10 and +20 degrees for towed model free to heave and pitch in Wave-1 ($a = 0.019$ m and $T = 1.254$ s).

- From an educational perspective, this enhanced insight is invaluable, particularly for the next generation of naval architects. It significantly deepens our understanding of how fundamental fluid dynamics govern ship powering, bridging the gap between theoretical principles and practical applications. This comprehensive approach equips future marine engineers with a robust grasp of core concepts, better preparing them for advanced challenges in the field.
- These tests are crucial as the shipping industry increasingly seeks to enhance its energy efficiency. Understanding how to better design hulls to operate at steady drift angles, especially when equipped with wind assist systems, is essential. Additionally, optimising bow and stern arrangements for operation in realistic sea states is vital. These improvements are key to reducing energy consumption and advancing sustainable practices within the maritime sector.
- Interpreting the relationships between actual energy supplied during specific wave encounters is crucial for evaluating the performance of energy-saving devices. This applies both at the model scale and in full-scale ship evaluations, where more comprehensive data sets are available. At the model scale, the ability to instrument electric motors and measure all power losses provides a clearer picture of where energy losses occur. This enhanced understanding supports a more informed approach to ship design, recognising that the addition of a simple power margin is no longer appropriate.
- The data collected from experiments will be crucial for elucidating how CFD can be reliably incorporated into ship design for operational sea states. By measuring force components on the hull, propeller, and rudder at the model scale, it is feasible to develop and refine scaling processes that accurately predict full-scale performance. This approach not only enhances the predictive capabilities of CFD simulations but also supports the development of more efficient and effective ship designs tailored to specific operational conditions.

In conclusion, this paper facilitates a better understanding of the ship's unsteady hydrodynamic performance in waves using experimental method by developing a highly instrumented self-propelled ship model capable of capturing time accurate performance both when towed and capable of free running in a towing tank, basin or in fresh water lakes. This investigation makes it possible to provide some good insights into better ship design by enhancing the understanding of the quality of resistance and powering data, how fundamental fluid dynamics controls ship powering, how the bow and stern arrangements can be optimised at steady drift angles when operating in realistic sea states. This study also provides clearer insights into energy supplied during specific wave encounters, enhancing understanding of how Energy Saving Devices (ESDs) and ships perform under varying sea conditions in terms of energy efficiency. Last but not least, the data obtained from this study are crucial for demonstrating how CFD can reliably contribute to ship design in operational sea conditions, allowing for the measurement of force components on hulls, propellers, and rudders at model scale, and developing scaling processes for full-scale performance predictions. Potential future work should include

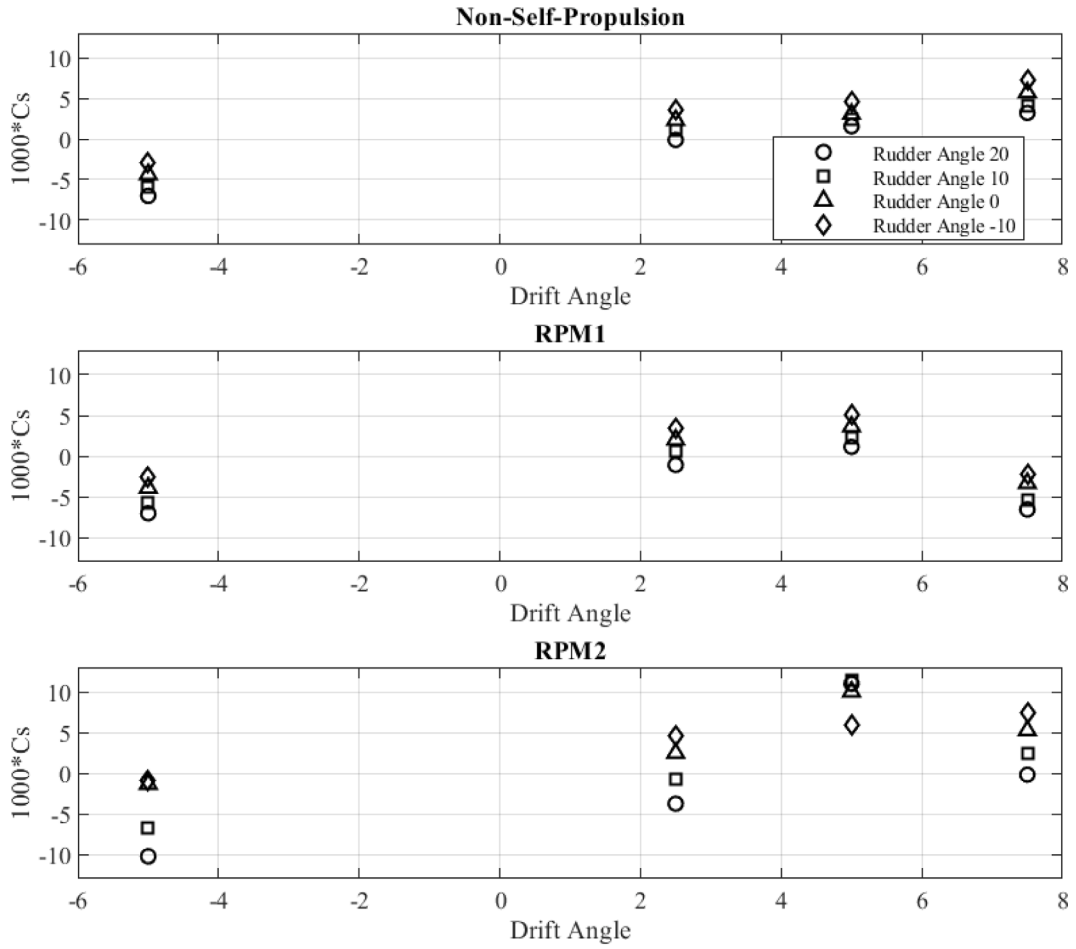

Fig. 16. Non-dimensional hull side-force for drift angles between −5 and +7.5 degrees and rudder angles between −10 and +20 degrees for towed model free to heave and pitch in Wave-2 ($a = 0.038$ m and $T = 1.667$ s).

the acquisition of free running manoeuvring tests in both regular and irregular waves, which can help achieve full validation and verification of dynamic ship manoeuvring simulation in waves.

CRediT authorship contribution statement

Stephen Turnock: Writing – review & editing, Supervision, Project administration, Methodology, Funding acquisition, Conceptualization. **Saeed Hosseinzadeh:** Writing – review & editing, Writing – original draft, Visualization, Investigation, Formal analysis. **Yifu Zhang:** Writing – review & editing, Writing – original draft, Visualization, Investigation, Formal analysis. **James Bowker:** Writing – original draft, Software, Methodology, Investigation, Conceptualization. **Dickon Buckland:** Software, Investigation, Data curation. **Magnus Gregory:** Software, Investigation, Data curation. **Nicholas Townsend:** Writing – review & editing, Methodology, Investigation.

Declaration of competing interest

The authors declare that they have no known competing financial interests or personal relationships that could have appeared to influence the work reported in this paper.

Data availability

The data for self-propulsion experiments in calm water and waves is available in Hosseinzadeh et al. (2024a), with detailed instructions for using the dataset provided in (Hosseinzadeh et al., 2024b). All other data will be made available upon request.

Acknowledgements

The authors acknowledge the support of the first-year cohort of students of SESS6077 for their participation in testing a new approach to ship power laboratories. Funding for the development of the KCS hull was supplied by the School of Engineering and the instrumentation fitout was part of the Clean Maritime Demonstration project AMPS-USV as well as Winds of Change project of Innovate UK. The expertise of Boldrewood towing tank staff Bertrand Malas and David Turner was vital.

References

Badoe, C., 2015. Design Practice for the Stern Hull of a Future Twin-Skeg Ship Using a High Fidelity Numerical Approach (Ph.D. thesis). University of Southampton.

Bassam, A.M., Phillips, A.B., Turnock, S.R., Wilson, P.A., 2019. Experimental testing and simulations of an autonomous, self-propulsion and self-measuring tanker ship model. Ocean Eng. 186, 106065.

Bowker, J., Buckland, D., Gregory, M., Townsend, N., Zhang, Y., Turnock, S., 2023. A free running instrumented container ship model for investigating energy efficiency in waves.

Gorski, J.J., 2002. Present state of numerical ship hydrodynamics and validation experiments. J. Offshore Mech. Arct. Eng. 124 (2), 74–80.

Hino, T., Stern, F., Larsson, L., Visonneau, M., Hirata, N., Kim, J., 2020. Numerical Ship Hydrodynamics: An Assessment of the Tokyo 2015 Workshop. Vol. 94, Springer Nature.

Hirdaris, S., Bai, W., Dessi, D., Ergin, A., Gu, X., Hermundstad, O., Huijsmans, R., Iijima, K., Nielsen, U.D., Parunov, J., et al., 2014. Loads for use in the design of ships and offshore structures. Ocean Eng. 78, 131–174.

Hirdaris, S., Temarel, P., 2009. Hydroelasticity of ships: recent advances and future trends. Proc. Inst. Mech. Eng. M 223 (3), 305–330.

Hosseinzadeh, S., Tabri, K., Topa, A., Hirdaris, S., 2023. Slamming loads and responses on a non-prismatic stiffened aluminium wedge: Part II. Numerical simulations. Ocean Eng. 279, 114309.

Hosseinzadeh, S., Turnock, S., Lee, H., Olvera, R., 2024a. Dataset in support of the paper'experimental dataset of a model-scale ship in calm water and waves'. http://dx.doi.org/10.5258/SOTON/D3076, URL: http://eprints.soton.ac.uk/id/eprint/490226.

Hosseinzadeh, S., Turnock, S., Lee, H., Olvera, R., 2024b. Experimental dataset of a model-scale ship in calm water and waves. Available at SSRN 4851029. URL: http://dx.doi.org/10.2139/ssrn.4851029.

ITTC, 2008. Guidelines. Testing and extrapolation methods. High speed marine vehicles resistance test. In: Proceedings of the 25th ITTC, Fukuoka, Japan. pp. 14–20.

ITTC, 2011. Recommended Procedures and Guidelines: Resistance Test. Rev 3. 7.5-02-02-01.

ITTC, 2017. Recommended procedures and guidelines: Resistance and propulsion test and performance prediction with skin frictional drag reduction techniques.

Köksal, Ç., Aktas, B., Gürkan, A., Korkut, E., Sasaki, N., Atlar, M., 2022. Experimental powering performance analysis of M/V ERGE in calm water and waves. In: A. Yücel Odabaşı Colloquium Series 4th International Meeting-Ship Design & Optimization and Energy Efficient Devices for Fuel Economy. Istanbul, Türkiye.

Krasilnikov, V., Ponkratov, D., Crepier, P., 2011. A numerical study on the characteristics of the system propeller and rudder at low speed operation. In: Second International Symposium on Marine Propulsors. SMP11, Hamburg, Germany.

Larsson, L., Stern, F., Visonneau, M., 2013. Numerical Ship Hydrodynamics: An Assessment of the Gothenburg 2010 Workshop. Springer.

Lee, H., 2023. Experimental Investigation of Wind-Assisted Ship Performance in Waves and Its Impact on the Interaction Between Hull, Propeller, and Rudder (Ph.D. thesis). University of Southampton.

Lee, Y.-G., Yu, J.-W., Kang, B.-H., Pak, K.-R., 2008. A numerical study on the flow around a rudder behind low speed full ship. J. Ship Ocean Technol. 12 (2), 41–52.

Malas, B., Creasey, L., Buckland, D., Turnock, S.R., 2024. Design, development and commissioning of the Boldrewood towing tank–a decade of endeavour. Int. J. Marit. Eng. 165 (A3 (2023)), A–255.

MEPC72, I., 2018. Resolution MEPC. 304 (72). In: Initial IMO Strategy on Reduction of GHG Emissions from Ships.

Molland, A.F., Turnock, S.R., 2011. Marine Rudders and Control Surfaces: Principles, Data, Design and Applications. Elsevier, http://dx.doi.org/10.1016/B978-0-7506-6944-3.X5000-8.

Molland, A.F., Turnock, S.R., Hudson, D.A., 2017. Ship resistance and propulsion. Cambridge university press, http://dx.doi.org/10.1017/9781316494196.

Papanikolaou, A., 2010. Holistic ship design optimization. Comput. Aided Des. 42 (11), 1028–1044.

Phillips, A.B., Turnock, S.R., Furlong, M., 2010. Accurate capture of propeller-rudder interaction using a coupled blade element momentum-RANS approach. Ship Technol. Res. 57 (2), 128–139.

Sanada, Y., Park, S., Kim, D.-H., Wang, Z., Stern, F., Yasukawa, H., 2021. Experimental and computational study of hull–propeller–rudder interaction for steady turning circles. Phys. Fluids 33 (12).

Stern, F., Agdraup, K., Kim, S., Hochbaum, A., Rhee, K., Quadvlieg, F., Perdon, P., Hino, T., Broglia, R., Gorski, J., 2011. Experience from SIMMAN 2008—the first workshop on verification and validation of ship maneuvering simulation methods. J. Ship Res. 55 (02), 135–147.

Tacar, Z., Sasaki, N., Atlar, M., Korkut, E., 2020. An investigation into effects of gate rudder® system on ship performance as a novel energy-saving and manoeuvring device. Ocean Eng. 218, 108250.

Temarel, P., Bai, W., Bruns, A., Derbanne, Q., Dessi, D., Dhavalikar, S., Fonseca, N., Fukasawa, T., Gu, X., Nestegård, A., et al., 2016. Prediction of wave-induced loads on ships: Progress and challenges. Ocean Eng. 119, 274–308.

Tezdogan, T., Demirel, Y.K., Kellett, P., Khorasanchi, M., Incecik, A., Turan, O., 2015. Full-scale unsteady RANS CFD simulations of ship behaviour and performance in head seas due to slow steaming. Ocean Eng. 97, 186–206.

Wang, J., Zou, L., Wan, D., 2018. Numerical simulations of zigzag maneuver of free running ship in waves by RANS-overset grid method. Ocean Eng. 162, 55–79.

Woeste, J.T., O'Reilly, C.M., Gouveia, R.K., Young, Y.L., 2022. Propeller–hull interactions and added power in head seas. Ocean Eng. 247, 110630.

Yilmaz, N., Aktas, B., Atlar, M., Fitzsimmons, P.A., Felli, M., 2020. An experimental and numerical investigation of propeller-rudder-hull interaction in the presence of tip vortex cavitation (TVC). Ocean Eng. 216, 108024.

Zhang, Y., 2023. Influence of Drift Angle on the Self-Propelled Ship's Powering Performance in Waves (Ph.D. thesis). University of Southampton, URL: https://eprints.soton.ac.uk/483454/.

Zhang, Y., Hosseinzadeh, S., Banks, J., Hudson, D., Turnock, S., 2023. Influence of leeway on hull-propeller-rudder interaction using CFD methods. http://dx.doi.org/10.15480/882.9333.

Zhang, Y., Hudson, D., Winden, B., Turnock, S., 2021. Evaluating the effects of drift angle on the self-propelled ship using blade element momentum theory. URL: https://eprints.soton.ac.uk/452646/.

Zhang, Y., Winden, B., Hudson, D., Turnock, S., 2022. Hydrodynamic performance of a self-propelled KCS at angle of drift including rudder forces. URL: https://eprints.soton.ac.uk/474374/.

Zhang, Y., Windén, B., Ojeda, H.R.D., Hudson, D., Turnock, S., 2024. Influence of drift angle on the propulsive efficiency of a fully appended container ship (KCS) using computational fluid dynamics. Ocean Eng. 292, 116537, URL: https://doi.org/10.1016/j.oceaneng.2023.116537.